Biophysical Chemistry 172 (2013) 61–67

Contents lists available at SciVerse ScienceDirect

Biophysical Chemistry

journal homepage: http://www.elsevier.com/locate/biophyschem

Thermodynamic parameters of anion binding to halorhodopsin from *Natronomonas pharaonis* by isothermal titration calorimetry

Saori Hayashi [a], Jun Tamogami [b], Takashi Kikukawa [c], Haruka Okamoto [b], Kazumi Shimono [b,1], Seiji Miyauchi [b,1], Makoto Demura [c], Toshifumi Nara [b], Naoki Kamo [a,b,c,*]

[a] *Graduate School of Pharmaceutical Sciences, Hokkaido University, Sapporo 060-0812, Japan*
[b] *College of Pharmaceutical Sciences, Matsuyama University, Matsuyama 790-8578, Japan*
[c] *Faculty of Advanced Life Science, Hokkaido University, Sapporo 060-0810, Japan*

HIGHLIGHTS

- The thermodynamic parameters of anion binding to halorhodopsin were determined.
- The dilution heat was minimalized by considering water activities.
- K_d values were almost equal to those determined by the conventional spectroscopy.
- The protonated Schiff base was essential for the anion binding.

GRAPHICAL ABSTRACT

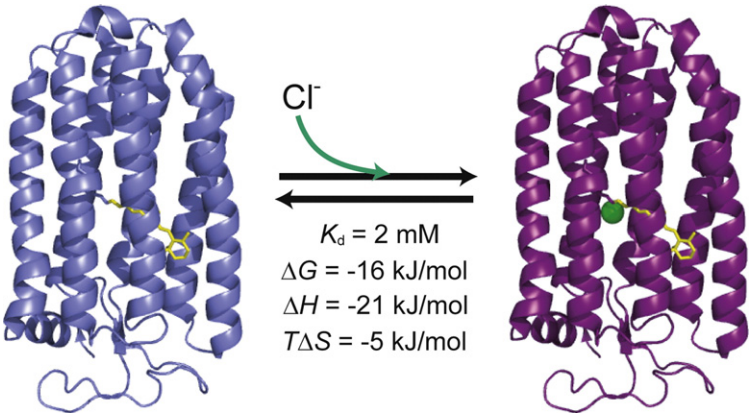

ARTICLE INFO

Article history:
Received 8 November 2012
Received in revised form 10 January 2013
Accepted 14 January 2013
Available online 20 January 2013

Keywords:
Microbial rhodopsin
ITC
Anion binding
Thermodynamic parameters
Opsin

ABSTRACT

Halorhodopsin (HR), an inwardly directed, light-driven anion pump, is a membrane protein in halobacterial cells that contains the chromophore retinal, which binds to a specific lysine residue forming the Schiff base. An anion binds to the extracellular binding site near the Schiff base, and illumination makes this anion go to the intracellular channel, followed by its release from the protein and re-uptake from the opposite side. The thermodynamic properties of the anion binding in the dark, which have not been previously estimated, are determined using isothermal titration calorimetry (ITC). For Cl^- as a typical substrate of HR from *Natronomonas pharaonis*, $\Delta G = -RT \ln(1/K_d) = -15.9$ kJ/mol, $\Delta H = -21.3$ kJ/mol and $T\Delta S = -5.4$ kJ/mol at 35 °C, where K_d represents the dissociation constant. In the dark, K_d values have been determined by the usual spectroscopic methods and are in agreement with the values estimated by ITC here. Opsin showed no Cl^- binding ability, and the deprotonated Schiff base showed weak binding affinity, suggesting the importance of the positively charged protonated Schiff base for the anion binding.

Abbreviations: HR, halorhodopsin; BR, bacteriorhodopsin; NpHR, halorhodopsin from *Natronomonas pharaonis*; HsHR, halorhodopsin from *Halobacterium salinarum*; λ_{max}, absorption maximum; ITC, isothermal titration calorimeter; K_d, dissociation constant; K_b, binding constant ($=1/K_d$); DDM, *n*-dodecyl-β-D-maltoside; PC, L-α-phosphatidylcholine; MES, 2-(*N*-morpholino)ethanesulfonic acid; EC, extracellular channel; CP, cytoplasmic channel.

* Corresponding author at: Faculty of Advanced Life Science, Hokkaido University, Sapporo 060-0810, Japan. Tel.: +81 11 706 3435; fax: +81 11 624 6337.
E-mail address: nkamo@pharm.hokudai.ac.jp (N. Kamo).
[1] Present address: Faculty of Pharmaceutical Sciences, Toho University, Funabashi 274-8510, Japan.

0301-4622/$ – see front matter © 2013 Elsevier B.V. All rights reserved.
http://dx.doi.org/10.1016/j.bpc.2013.01.001

1. Introduction

Halorhodopsin (HR) is an inwardly directed light-driven Cl^--pump in halobacterial cell membranes [1–5]. The transfer of negative charges across the membrane by HR induces the inside-negative membrane potential that increases the proton-motive force created by bacteriorhodopsin (BR), an outwardly directed light-driven proton-pump in the same halobacterial membranes [6–8]. Like the well-known BR, HR is a seven-helix membrane protein, and retinal binds to a specific lysine residue in the 7th (G) helix via the protonated Schiff base [9]. Since retinal works as a chromophore, this binding affords the visible light absorption whose absorption maximum (λ_{max}) is ~580 nm. Absorption of a photon initiates the photocycle in which the excited HR relaxes to the original ground state via a series of various photo-intermediates referred to as K, L, N and O [4,10–13]. During the transition from N to O intermediate, one Cl^- is released to the intracellular space, and during the transition from O to HR, another Cl^- enters from the opposite side, i.e., the extracellular space [14–17]. Thus, by the completion of the photocycle, one Cl^- transfers from the outside to the inside of cells.

In the unphotolyzed state, Cl^- binds to the binding site located near the positively charged protonated Schiff base in the extracellular channel [18,19]. This binding affinity has been estimated from the spectrum shift of Cl^- titration. For instance, the Cl^- binding to the Cl^--free form of HR from *Natronomonas pharaonis* gives rise to the blue shift of λ_{max} from ~600 (anion-free form) to 580 nm (the bound form) [12,20]. This shift is interpreted to be the stabilization of the ground state energy level due to the electrostatic interaction between the positively charged protonated Schiff base and the negatively charged anion. Analysis of this spectrum shift gives a value of several mM for the dissociation constant, K_d, of HR.

In this paper, we intended to obtain K_d values of the anion binding with another method such as isothermal titration calorimeter (ITC). However, two problems arise. The first problem is that for the precise determination of binding constants ($K_b = 1/K_d$) with the manufacturer's analysis software, the c value, which is defined as $c = K_b \cdot M_{tot} \cdot n$, where M_{tot} and n represent the sample concentration and the stoichiometry number, respectively, should be in the range of 1–1000. Because, as described above, $K_b \sim 1/5\ mM^{-1}$, M_{tot} should be in the range of 5 mM–5 M (assuming $n = 1$). The preparation of such a high concentration of protein solutions, however, is impossible. Obviously, this problem is due to the fundamentally weak interactions, as manifested in the large values of K_d. The other problem is the production of the dilution heat. Due to the large K_d values, a high concentration of Cl^- is required for the injection solution, which yields appreciable dilution heat at the titration. We found a method to avoid these problems and succeeded in the estimation of K_d values and thermodynamic parameters. Values of K_d estimated by this method were similar to those determined from the λ_{max}-shift. Suggestions on the existence of the other binding sites have been reported [21,22] which may not affect the absorption of HR, and then analysis in this paper was carried out on assumption that there are strong and weak binding sites. The thermodynamic parameters associated with anion binding to HR (strong binding) were first reported in this paper. It is noteworthy that anions do not bind to opsin, a protein part of rhodopsin only without retinal, showing the important role of the positively charged protonated Schiff base in anion binding. This finding was not obtained by the spectroscopic method and was first obtained here by the ITC method.

2. Materials and methods

2.1. Preparation of NpHR

Previous investigation of HR has been performed using two sources. One source is *Halobacterium salinarum*, and the other is *Natronomonas pharaonis* (abbreviated as NpHR). NpHR was used in this study because the expression system using *Escherichia coli* has been established [23,24]. Expression of the (6×) histidine-tagged protein and purification procedures using *E. coli* BL21(DE3) cells harboring the appropriate plasmid were performed as described elsewhere [24,25]. The binding was measured not only for the wild-type but also for various mutants. Given that charged or hydrophilic amino acid residues may play an important role, we made mutants of Arg123, Thr126 and Ser130, which are all located near the binding site in the extracellular channel. In addition, mutants of Lys215 and Thr218 in the cytoplasmic channel were prepared. The construction of these mutants was described in Sato et al. [26–28] and Kubo et al. [29]. The opsin (with a 6× his-tag) was prepared without an addition of retinal at the induction and purified as usual. The protein was solubilized with 0.1% *n*-dodecyl-β-D-maltoside (DDM, from Dojindo, Kumamoto, Japan). The protein concentration was determined using the extinction coefficient of 54,000 at 578 nm in the presence of Cl^- and 50,000 in the absence of Cl^-[20]. For opsin, a large enough amount of retinal was added after the experiment to estimate the concentration by the absorption.

2.2. Reconstitution of NpHR with phospholipids

The sample was reconstituted with phospholipids to increase the stability of NpHR and to make buffer exchange easier. The protein solubilized with 0.1% DDM and L-α-phosphatidylcholine (PC) from egg york (Funakoshi, Tokyo, Japan) was mixed at a molar ratio of 1:50. DDM was removed with biobeads SM2 (1 g for 1 ml of 1% DDM, BIO-RAD, Tokyo) under a nitrogen atmosphere at 4 °C. Details are described elsewhere [30,31].

2.3. ITC measurements

A VP-ITC (MicroCalorimeter, MicroCal, Northampton, MA) was used. PC-reconstituted NpHR solutions of 30–50 μM were added into the lower cell chamber (1.45 mL), and the injection syringe contained a concentrated salt solution whose compositions are shown below. The NpHR sample in the lower cell was suspended in 500 mM 2-(*N*-morpholino) ethanesulfonic acid (MES) adjusted to a pH of 6.0. The dissociation of the protonated Schiff base of the Cl^--free NpHR was observed in alkali solutions, and experiments were carried out at pH 6. The solution compositions of the injection syringe were dependent on the salt used. These compositions were determined by a trial-and-error method so that the dilution heat became minimal. Compositions used were as follows:

NaCl, 150 mM NaCl, 475 mM MES, pH 6.0

NaBr, 150 mM NaBr, 450 mM MES, pH 6.0

NaI, 150 mM NaI, 490 mM MES, pH 6.0

$NaNO_3$ 150 mM $NaNO_3$, 420 mM MES, pH 6.0

NaSCN 150 mM NaSCN, 475 mM MES, pH 6.0

The reason of variations of MES concentrations on anion species is not clear. As described above, these titration solutions having these MES concentrations yielded the smallest dilution heat. Since as described below, the volumes added from the syringe are at most 250 μL (5 μL×50 times) and the lower cell contained 1.45 mL of 500 mM of MES, the ionic strength variations in the cell depending on anion species used were small.

Prior to ITC measurements, both the sample protein and injection solutions were de-gassed with ThermoVac Sample Degassing and Thermostat (MicroCal, Northampton, MA). The temperature was set to 35 °C. The protein solution in the cell was stirred at 300 rpm. The duration and spacing of injection were 10 s and 240 s, respectively. The numbers of injections were either 30 or 50. The first injection volume was 2.5 μL, and the volume increased to 5.0 μL due to the second injection.

The accumulation of the heat-flow was calculated with a custom algorithm using Excel (Microsoft, Seattle).

2.4. Estimation of the K_d by the spectroscopic titration method

Spectroscopic titration was performed to obtain K_d values of NpHR in the medium used here and for comparison with the values estimated by the ITC method. For this procedure, DDM-solubilized samples in 500 mM MES (pH 6.0) containing 0.05% DDM were used instead of the lipid-reconstituted sample, which showed excessive scattering that prevented spectroscopic measurements. The spectrophotometer used was the Hitachi U-3310 (Tokyo, Japan). The temperature used (35 °C) was the same as that used for ITC. The analysis was performed via the following equation:

$$\Delta A = \Delta A_{\max} \frac{[Anion]}{K_d + [Anion]}$$

where ΔA and ΔA_{max} represent the absorbance changes due to the anion binding and the maximum absorbance changes, respectively. As described above, the anion binding to the anion-free NpHR results in a blue-shift of the spectra, resulting in a decrease in the absorbance at longer wavelengths. ΔA in the above equation was measured at 633 nm for Cl^-, 635 nm for Br^-, 634 nm for I^-, 622 nm for NO_3^- and 627 nm for SCN^-. The dilution caused by the addition of anion solutions was corrected.

Váró et al. [14] measured flash-induced absorbance changes of NpHR at 500, 590 and 640 nm. In the absence of Cl^-, they observed small absorbance changes at 500 nm (due to the L-intermediate) whose amplitudes were increased with an increase in Cl^- concentration. In addition, the flash-induced Cl^--dependent absorbance changes (absolute values) of these three wavelengths were almost the same, and these changes accorded with the spectrum change of unphotolyzed NpHR. The media contained various ratios of NaCl and Na_2SO_4 to keep the ionic strength constant. We confirmed these (data not shown). Hence we estimated the K_d value from the L-yields by flash photolysis in varying Cl^- concentrations when the basic media contained 500 mM MES (pH 6). The apparatus and procedure for the flash-photolysis were the same as that reported previously [25].

3. Results and discussion

3.1. Selection of media for ITC experiments

Because the K_d value is several mM, the concentration of the injection salt solution was high. We employed 150 mM injection solutions, which resulted in final concentrations of 15 mM or 24 mM after 30 or 50 injections, respectively. The problem was to prevent the heat production due to the dilution with injection. As anticipated, non-negligible heat production was observed when the protein solution dissolved in an ordinary buffer was titrated by the high concentration salt solution. After preliminary experiments, we noticed that equal activities of water in the protein solution and the injection solution may be crucial because water is the major component. Because the injection solution contained a high salt concentration, the protein solution in the lower cell also required a high salt concentration. This necessity of a high ionic concentration favored the stability of NpHR. The first injection solution tried was sodium sulfate. Sulfate is known as an anion that does not bind to the binding site near the Schiff base, and thus, this anion does not induce the spectrum shift. A sulfate anion may bind to another binding site of HR from *Halobacterium salinarum* (HsHR), but this binding does not induce the spectrum shift, potentially because this site is far from the chromophore [32]. To avoid the possible interaction of NpHR with a sulfate anion, we employed MES solutions. Such a large anion may not interact with HR. The anion concentration in the injection syringe was as high as 150 mM sodium solution. Therefore, as described above, to equalize the water activities as much as possible in both the solutions of the cell and injector syringe, a high concentration of MES (500 mM) was employed. After several trial-and-error examinations, it was possible to determine the best compositions of the injection solutions, which are described in Materials and methods (also see the legend to Fig. 1). It is noted that the MES concentrations are dependent on the anions used.

3.2. Analysis of ITC data: Estimation of the dissociation constant K_d and thermodynamic parameters of the anion binding

Typical data are shown in Fig. 1 in which the heat-flow of 2 in the upper panel is Cl^- titration data showing an exothermic binding, while the heat-flow of 1 is the data obtained without the protein, revealing the negligibly small dilution heat. Analysis of the titration data is based on a very simple idea in which the accumulation of the time integration of the heat-flow should yield a binding isotherm. Panel b in Fig. 1 shows the binding isotherm calculated from this integration. The heat production without NpHR (heat-flow 1) in Fig. 1 was subtracted from those of heat-flow 2 to calculate the net heat production by the binding. Because the injection volume was 5 μL per injection and the cell volume was 1.45 mL, the 50- or 30-time titration resulted in a final volume increase of 17.2% or 10.3%, respectively. This increase in the volume was ignored. Panel b in Fig. 1 suggests that the binding does not follow a single binding equation and more likely demonstrates the existence of a weak binding site, as is described in introduction. Thus, we assumed the following equation for fitting, where the NpHR concentration of the anion-bound form, C_b, should be:

$$C_b = C_{b,s} + C_{b,w}$$

where the subscripts s and w signify the strong and weak binding, respectively. As to the strong binding, the following equation holds:

$$K_d = \frac{[free\,HR\,binding\,site][free\,anion]}{[bound\,site]} = \frac{\left(n \cdot C_P - C_{b,s}\right) C_{anion,f}}{C_{b,s}}$$

where n,C_p and $C_{anion,f}$ signify the number of binding sites per molecule of NpHR, the NpHR concentration and the concentration of free anion, respectively. Rearrangement of this equation yields the following familiar equation:

$$C_{b,s} = \frac{nC_p \cdot C_{anion,f}}{K_d + C_{anion,f}}$$

For the present system, the binding is weak (K_d~2 mM) and the NpHR concentration is *ca.* 30–50 μM. Therefore, the concentration of the bound anion is negligible in comparison with the total anion concentration in the cell. Fortunately, this led to the simple equation where $C_{anion,f}$ is approximately equal to the total concentration of anion, C_{anion}. Thus, the above equation is rewritten as:

$$C_{b,s} = \frac{nC_p \cdot C_{anion}}{K_d + C_{anion}}$$

The values of C_{anion} were calculated from the total added volume due to injection. For the weak binding component, we assumed linear binding, which reduced the number of unknown parameters. Thus, using a as a linear binding coefficient,

$$C_{b,w} = a \cdot C_p \cdot C_{anion}$$

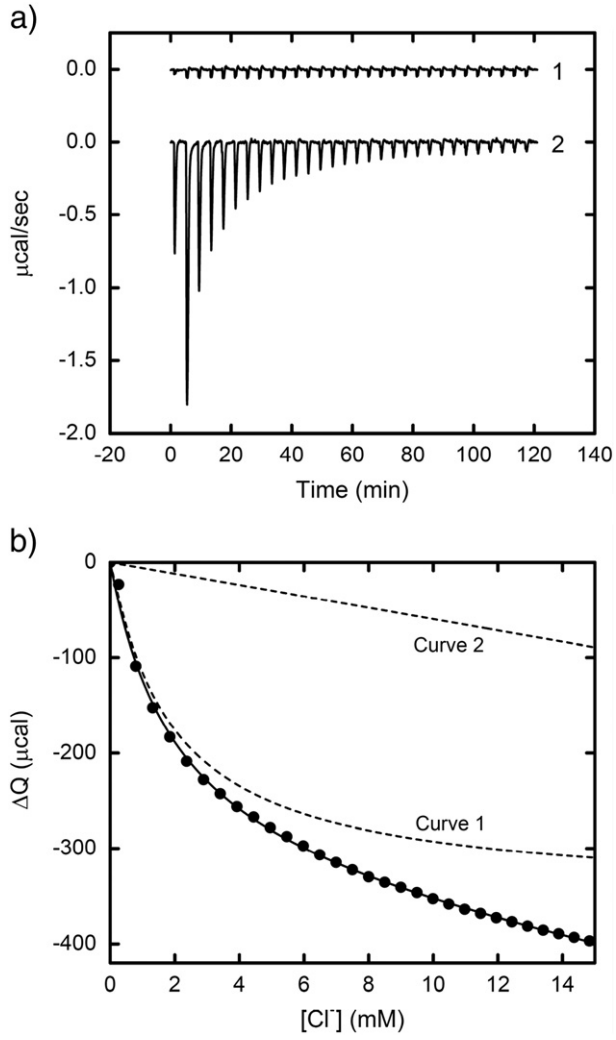

Fig. 1. Isothermal titration calorimetry data of the binding of chloride to NpHR. Panel a); Raw ITC data. Heat-flow 2 shows heat flow data of NpHR. Lipid-reconstituted NpHR (47.4 μM) was suspended in 500 mM MES (pH 6.0), 1.45 mL of which was used as sample solution in the lower chamber. The injection buffer was composed of 150 mM NaCl and 475 mM MES (pH 6.0). The titration was carried out by stepwise 30-count additions of 5 μL (except for 2.5 μL for the first injection). The time interval between successive injections was 240 s. The temperature was 35 °C. Heat-flow 1 shows only a small heat production due to the mixing of two buffers. Panel b); One data analysis example. The heat-flow (generation) was calculated by (heat-flow 2) − (heat-flow 1) in panel a), integrated, and this integrated value was accumulated. The accumulated heat-flows are plotted against the concentration of Cl^- in the cell that was increased by the injections. The data points thus obtained were fit by Eq. (1) with a non-linear regression. The thick line is the resulting curve fit, expressed by Eq. (2). Curve 1 represents the first term in the right-hand side of Eq. (2) (tight binding), and Curve 2 represents the second term (non-specific binding).

Therefore, we obtained the following equation of the accumulated heat produced, ΔQ:

$$\Delta Q = \left(\Delta H_s \cdot C_{b,s} + \Delta H_w \cdot C_{b,w}\right) \cdot V_c = \left(\Delta H_s \cdot \frac{nC_p \cdot C_{anion}}{K_d + C_{anion}} + \Delta H_w \cdot a \cdot C_p \cdot C_{anion}\right) \cdot V_c \quad 1$$

where V_c means the volume of the cell (1.45 mL).

Fitting Eq. (1) to the data shown in Panel b of Fig. 1 gave

$$\Delta Q = \frac{-350\,(\mu cal) \cdot C_{Cl}}{2.0(mM) + C_{Cl}} - 5.96(\mu cal) \cdot C_{Cl} \quad 2$$

In Panel b, curve 1 represents the first term on the right-hand side of Eq. (2), and curve 2 represents the second term.

Assuming that $n = 1$ in Eq. (1) (see below), from Eq. (2), we obtained

$$\Delta H_s = \frac{-350(\mu cal)}{C_p \cdot V_c} = -\frac{350(\mu cal)}{47.4(\mu M) \cdot 1.45(mL)} = -5.09 \text{ kcal/mol} = -21.3 \text{ kJ/mol}.$$

Because $K_d = 2.0$ mM (see Eq. (2)), the Gibbs energy change, ΔG_s, and the entropy change, ΔS_s, are calculated as follows:

$$\Delta G_s = -RT \ln \frac{1}{2.0 \times 10^{-3}} = -15.9 \text{ kJ/mol}.$$

$$\Delta S_s = \frac{\Delta H - \Delta G}{T} = \frac{-21.3 - (-15.9)}{308} = -17.5\, J/(K \cdot mol)$$

The ITC experiment was performed at varying protein concentrations (30–50 μM), but the values obtained were independent of this concentration. Moreover, similar values were obtained for 0.1% DDM-solubilized samples.

Thus, the binding is enthalpy-driven. The large negative value of ΔS_s may come from conversion of two molecules (NpHR and Cl^-) into one molecule. In addition, this large negative value might suggest a decrease in the flexibility of amino acid residues, especially in the vicinity of the Cl^- binding site, as X-ray structures of NpHR and HsHR showed an interaction of Cl^- with amino acid residues due to the formation of hydrogen bonds [18,19]. These interactions may cause the negative change in the enthalpy value. Replacing MES in the sample and injection solutions with glycerol 2-phosphate or BisTris (methane) did not appreciably change the values of ΔH. This finding may indicate that no proton movement occurs during the Cl^- binding because if proton movement occurs, the neutralization reaction may also occur, which is manifested in the differences in the observed ΔH values as a function of the buffer composition.

In the above calculation, we assumed $n = 1$ based on the X-ray structure of NpHR where one Cl^- anion binds to the binding site near the Schiff base [19]. The anion bound in this position is considered to be transported. In addition, another bound Cl^- anion was shown in the X-ray structure of NpHR [19]. NpHR forms a trimer structure, and this binding site is located between two adjacent NpHR molecules. Near the chloride ion, bacterioruberin squeezes into the NpHR molecules to make space for Cl^-. Because no bacterioruberin was present in the current experimental conditions, this binding site might not be produced. Therefore, it is probable that the weak binding in the second term of the right side of Eq. (1), expressed by the subscript w, is due to non-specific binding, although the possibility of binding at the second binding site is suggested [21,22].

As described above, the binding of anions to HR (both NpHR and HsHR) is usually determined by spectrum changes [11,12,20]. Fig. 2b shows the difference spectra induced by Cl^- titration. This figure indicates the largest changes at 633 nm; the absorbance changes at this wavelength are plotted against the Cl^- concentration. A K_d value of 1.6 mM was determined from this plot using the Langmuir isotherm. The same value was estimated to be 1.7 mM from the flash photolysis experiment (see panel d of Fig. 2). These values are very close to the value determined by ITC (2 mM).

The binding of other anions was also examined, and the results obtained are listed in Table 1. This table indicates the good agreement of the K_d values between the two methods (spectroscopy and ITC) except for when using NO_3^-. The reason for the difference with the nitrate anion relative to the other options is not known. In addition, the small $T\Delta S$ (absolute) and ΔH (absolute) values of the NO_3 anion are notable. It is known that D85T and D85S mutants of BR work as a light-driven anion pump similar to HR [33–35]. The guanidium of Arg82 of the anion-free D85S mutant orients to the EC (extracellular channel) side in the dark, while that of the Br-bound form orients to the Schiff base, i.e., to the opposite side [36,37]. Thus, rotation of the guanidium occurs, and the bound Br anion is sandwiched between the protonated Schiff

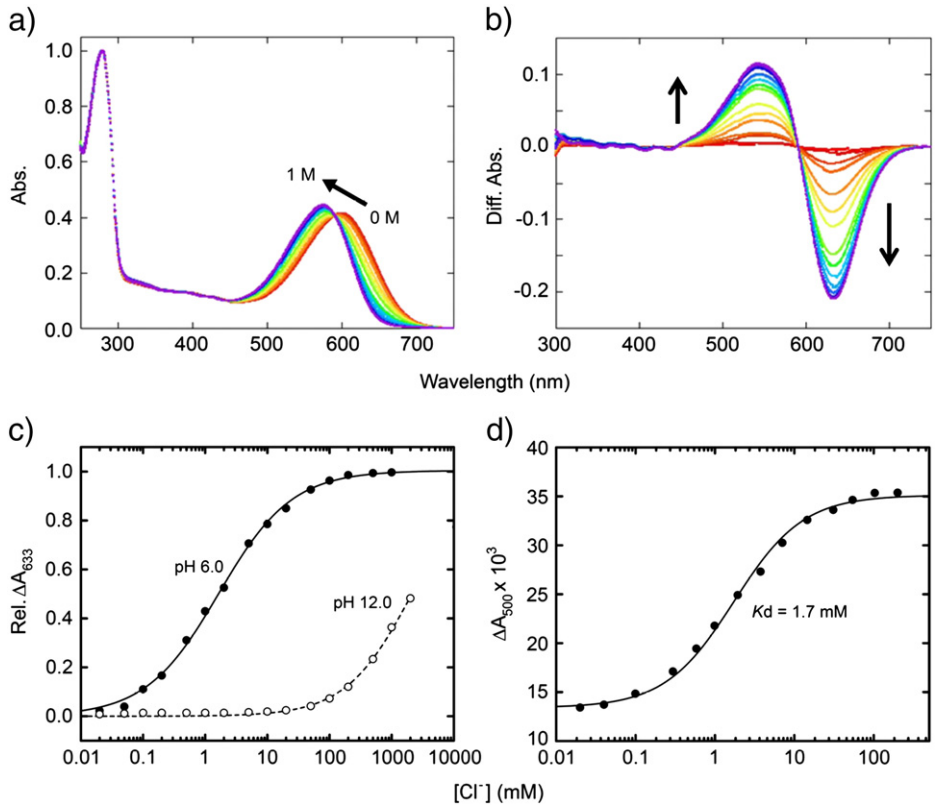

Fig. 2. Estimation of the K_d value of Cl^- binding based on the shift of the absorption maximum and the yield of the flash-induced L-intermediate formation. Panel a); 7.1 μM NpHR was suspended in 500 mM MES at 35 °C. The absorption spectra were measured under varying concentrations of Cl^-, showing the blue shift with an increase in the Cl^- concentration. Panel b); the difference spectra between the spectra shown in Panel a) and the spectrum of the Cl^--free form used as a reference. The largest changes in the difference spectra were obtained at 633 nm. Panel c); the absorbance differences at 633 nm of Panel b) are plotted against the Cl^- concentration. The absolute values are negative (ΔA decreases with an increase in Cl^- concentration). Closed circle symbols are those at pH 6, and open circle symbols are at pH 12. Panel d); the yields of laser-flash-induced L-intermediate formation (absorbance changes at 500 nm) are plotted against the Cl^- concentration. From this plot, the K_d value was estimated to be 1.7 mM.

base and the guanidium. On the other hand, the binding of NO_3^- does not change the orientation relative to that of the anion-free form, and the distance between the guanidium and the anion is larger with binding [38]. Thus, the electrostatic interaction of the positively charged guanidium with the bound NO_3^- anion may be smaller than that interaction when using Br^-. If the same situation occurs for the present NpHR-NO_3^-, it may explain the small ΔH, although the difference in the K_d values between the two methods is not clear. In addition the relatively large ion size of NO_3^- and the distribution of negative charge within NO_3^- molecule may be taken into consideration.

The importance of the Arg123 residue of NpHR and that of the corresponding residue of HsHR for the transport function has been reported [28,29,39,40]. In addition, other residues (Thr126 and Ser130) were reported to be important for the anion binding, as determined by the spectroscopic method [26,27]. Thus, the ITC experiments were carried out for mutants of these residues, and the results are shown in Fig. 3. All mutants showed smaller exothermic changes relative to the wild-type, which may be caused by weak interaction of NpHR mutants with Cl^-. Interestingly, a previous paper reported no Cl^--induced spectral changes for R123Q and R123H [28,29], while heat production was obtained for R123Q in the present ITC experiment. This suggests that there is a relatively strong Cl^- binding/interaction site in R123Q (not in R123H and R123K) other than the site near Schiff base. According to the crystal structure of NpHR [19], there are two Cl^- binding sites: One is proximity of Schiff base which affects the spectrum change, while the other is located at the interface of molecules within the trimer. The latter, however, may not exist because of the absence of bacterioruberin (see above) in the present experiments. Moverat-Kaplan [22] suggested the presence of the binding site (K_d ~100 mM) located on the EC (extracellular) channel where R123 residue is also located. Thus, there is a possibility that in R123Q, this binding site become stronger. Another point to be paid attention is that why the binding is weak for R123K although Lys bears positive charge as Arg. These are the subject for further investigation. In spite of these unsolved problems, the present results confirm that Arg123, Thr126 and Ser130 are important residues for the binding of anions to NpHR. Arg123 may contribute to the binding via electrostatic interaction, while Thr126 and Ser130 may contribute via hydrogen bonding.

Table 1
K_d values of anion binding to NpHR and their thermodynamic values.

Anion	$K_d^{1)}$ (mM)	$K_d^{2)}$ (mM)	$\Delta G^{3)}$ (kJ/mol)	ΔH (kJ/mol)	$-T\Delta S$ (kJ/mol)
Cl^-	1.6	2.0	−15.9	−21.3	5.4
Br^-	1.0	1.6	−16.5	−17.4	0.9
I^-	4.1	4.0	−14.1	−15.8	1.7
NO_3^-	14.5	5.8	−13.2 −10.8[4)]	−12.6	−0.6 1.8[4)]
SCN^-	6.7	7.0	−12.7	−38.8	26.1

$K_d^{1)}$ is estimated from the difference spectra. $K_d^{2)}$ is from ITC. $\Delta G^{3)}$ is the Gibbs free energy change calculated from $K_d^{2)}$. The ΔG and $-T\Delta S$ followed by the superscript 4) are the corresponding values calculated from $K_d^{1)}$.

Some amino acid residues in the CP (cytoplasmic channel) known to be important for function are Lys215 and Thr218 [28]. Their importance was examined through the use of the K215Q, K215R and T218V mutants. The results obtained were almost the same as the results with the wild-type (data not shown), indicating that amino acid residues in the CP do not affect anion binding in the dark.

It is probable that the positively charged protonated Schiff base may contribute significantly to the anion binding because the anion binding

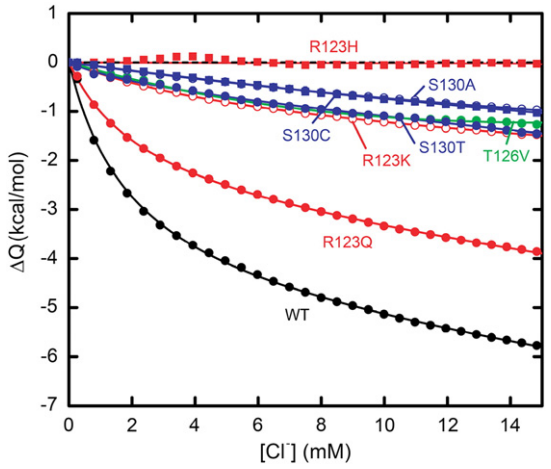

Fig. 3. ITC results of varying mutants of Arg123, Thr126 and Ser130. The accumulated heat-flows (production) are plotted against the Cl^- concentration. Each value was normalized by the amount of protein. The plots of mutants at the positions of Arg123, Thr126 and Ser130 are shown in red (R123Q;●, R123K;○, R123H;■), green (T126V;●) and blue (S130T;●, S130A;○, S130C;■), respectively, whereas those of WT are shown in black for comparison. The binding of mutant proteins was so weak that the analysis was not performed. This figure indicates the importance of Arg123, Thr126 and Ser130 for anion binding to NpHR and transport.

site is very close to the protonated Schiff base (3.46 Å) [19]. The experiment to examine whether the NpHR opsin can bind Cl^- was performed. Opsin is an only protein part of rhodopsin without retinal and then it does not contain Schiff base. The opsin concentration was 37.4 μM and the experimental procedures were the same in Fig. 1. Result (data not shown) indicates that either no binding occurred or that the K_d is much larger than the Cl^- concentration used in this experiment (up to 15.5 mM of Cl^-). This finding may indicate that the positively charged Arg123 is not sufficient for the Cl^- binding. It is noted that the examination of opsin binding should not be performed by the spectroscopic method but is possible by ITC. The next question is to examine the possibility of the binding to the deprotonated, neutral form of the Schiff base. The p*K*a value of the Schiff base was determined to be 11.7 in the presence of a high concentration of Cl^- (1 M) and 9.2 in the absence of Cl^- (data not shown). This value of 11.7 agrees with that of a reported value, but 9.2 is larger by nearly one unit than the value [41]. The difference may come from the difference in the media used. Therefore, at pH 12, the Schiff base of the Cl^--free NpHR is deprotonated (neutral form). The open circles in Fig. 2-c show the absorbance change at 633 nm when Cl^- titration was carried out at pH 12. This figure reveals no Cl^- binding until 100 mM Cl^- and absorbance changes occurs above 100 mM Cl^-, suggesting that NpHR with a deprotonated (neutral) Schiff base has weak affinity for anion binding. When negatively-charged Cl^- binds to the binding site near Schiff base, Schiff base will be forced to be the protonated form (positively charged) due to the electrical interaction, which results in the blue shift of absorbance. Since the pKa of Schiff base of the Cl^--bound form is 11.7, the protonated form can be present at pH 12 with amounts being about half. These observations suggest the importance of the positive charge of the protonated Schiff base. It is noted that the orientation change of the $N \rightarrow H^+$ dipole moment associated with the isomerization of retinal may be one of the driving forces behind the Cl^- movement from the EC binding site to the CP.

In conclusion the thermodynamic parameters of ΔH and ΔS due to anion binding to NpHR were first obtained experimentally. The ΔG's were calculated using K_d values determined by ITC data, which were almost equal to those determined by the widely-used spectroscopy method. In addition, some amino acid residues were confirmed via mutational analysis to play an important role in anion binding, and the importance of the positively charged Schiff base was suggested. Azide converts NpHR into a light-driven proton pump [41], and then the binding/interaction of azide with NpHR is an interesting subject, which will be a further investigation.

References

[1] A. Matsuno-Yagi, Y. Mukohata, Two possible roles of bacteriorhodopsin; A comparative study of strains of *Halobacterium halobium* differing in pigmentation, Biochemical and Biophysical Research Communications 78 (1977) 237–243.
[2] B. Schobert, J.K. Lanyi, Halorhodopsin is a light-driven chloride pump, Journal of Biological Chemistry 257 (1982) 10306–10313.
[3] J.K. Lanyi, Halorhodopsin, a light-driven electrogenic chloride-transport system, Physiological Reviews 70 (1990) 319–330.
[4] G. Váró, Analogies between halorhodopsin and bacteriorhodopsin, Biochimica et Biophysica Acta 1460 (2000) 220–229.
[5] L.O. Essen, Halorhodopsin: light-driven ion pumping made simple? Current Opinion in Structural Biology 12 (2002) 516–522.
[6] D. Oesterhelt, W. Stoecknius, Rhodopsin-like protein from the purple membrane of *Halobacterium halobium*, Nature: New Biology 233 (1971) 149–152.
[7] U. Haupts, J. Tittor, D. Oesterhelt, Closing in on bacteriorhodopsin: progress in understanding the molecule, Annual Review of Biophysics and Biomolecular Structure 28 (1999) 367–399.
[8] J.K. Lanyi, Bacteriorhodopsin, Annual Review of Physiology 66 (2004) 665–688.
[9] J.L. Spudich, C.-S. Yang, K.-H. Jung, E.N. Spudich, Retinylidene proteins: structures and functions from archaea to humans, Annual Review of Cell and Developmental Biology 16 (2000) 365–392.
[10] L. Zimányi, L. Keszthelyi, J.K. Lanyi, Transient spectroscopy of bacterial rhodopsins with an optical multichannel analyzer. 1. Comparison of the photocycles of bacteriorhodopsin and halorhodopsin, Biochemistry 28 (1989) 5165–5172.
[11] G. Váró, L. Zimányi, X. Fan, L. Sun, R. Needleman, J.K. Lanyi, Photocycle of halorhodopsin from *Halobacterium salinarium*, Biophysical Journal 68 (1995) 2062–2072.
[12] G. Váró, L.S. Brown, J. Sasaki, H. Kandori, A. Maeda, R. Needleman, J.K. Lanyi, Light-driven chloride ion transport by halorhodopsin from *Natronobacterium pharaonis*. 1. The photochemical Cycle, Biochemistry 34 (1995) 14490–14499.
[13] I. Chizhov, M. Engelhard, Temperature and halide dependence of the photocycle of halorhodopsin from *Natronobacterium pharaonis*, Biophysical Journal 81 (2001) 1600–1612.
[14] G. Váró, R. Needleman, J.K. Lanyi, Light-driven chloride ion transport by halorhodopsin from *Natronobacterium pharaonis*. 2. Chloride release and uptake, protein conformation change, and thermodynamics, Biochemistry 34 (1995) 14500–14507.
[15] E. Muneyuki, C. Shibazaki, H. Ohtani, D. Okuno, M. Asaumi, T. Mogi, Time-resolved measurements of photovoltage generation by bacteriorhodopsin and halorhodopsin adsorbed on a thin polymer film, Journal of Biochemistry 125 (1999) 270–276.
[16] K. Ludmann, G. Ibron, J.K. Lanyi, G. Váró, Charge motions during the photocycle of *pharaonis* halorhodopsin, Biophysical Journal 78 (2000) 959–966.
[17] C. Hasegawa, T. Kikukawa, S. Miyauchi, A. Seki, Y. Sudo, M. Kubo, M. Demura, N. Kamo, Interaction of the halobacterial transducer to a halorhodopsin mutant engineered so as to bind the transducer: Cl^- circulation within the extracellular channel, Photochemistry and Photobiology 83 (2007) 293–302.
[18] M. Kolbe, H. Besir, L.-O. Essen, D. Oesterhelt, Structure of the light-driven chloride pump halorhodopsin at 1.8 Å resolution, Science 288 (2000) 1390–1396.
[19] T. Kouyama, S. Kanada, Y. Takeguchi, A. Narusawa, M. Murakami, K. Ihara, Crystal structure of the light-driven chloride pump halorhodopsin from *Natronomonas pharaonis*, Journal of Molecular Biology 396 (2010) 564–579.
[20] B. Scharf, M. Engelhard, Blue halorhodopsin from *Natronobacterium pharaonis*: wavelength regulation by anions, Biochemistry 33 (1994), (6387-6393.K).
[21] D. Okuno, M. Asami, E. Muneyuki, Chloride concentration dependency of the electrogenic activity of halorhodopsin, Biochemistry 38 (1999) 5422–5429.
[22] K. Mevorat-Kaplan, V. Brumfeld, M. Engelhard, M. Scheves, The protonated Schiff base of halorhodopsin from *Natronobacterium pharaonis* is hydrolyzed at elevated temperature, Photochemistry and Photobiology 82 (2006) 1414–1421.
[23] I.P. Hohenfeld, A.A. Wegener, M. Engelhard, Purification of histidine tagged bacteriorhodopsin, *pharaonis* halorhodopsin and *pharaonis* sensory rhodopsin II functionally expressed in *Escherichia coli*, FEBS Letters 442 (1999) 198–202.
[24] M. Sato, T. Kanamori, N. Kamo, M. Demura, K. Nitta, Stopped-flow analysis on anion binding to blue-form halorhodopsin from *Natronobacterium pharaonis*: comparison with the anion-uptake process during the photocycle, Biochemistry 41 (2002) 2452–2458.
[25] M. Kubo, M. Sato, T. Aizawa, C. Kojima, N. Kamo, M. Mizuguchi, K. Kawano, M. Demura, Disassembling and bleaching of chloride-free *pharaonis* halorhodopsin by octyl-β-glucoside, Biochemistry 44 (2005) 12923–12931.
[26] M. Sato, T. Kikukawa, T. Araiso, H. Okita, K. Shimono, N. Kamo, M. Demura, K. Nitta, Ser-130 of *Natronobacterium pharaonis* halorhodopsin is important for the chloride binding, Biophysical Chemistry 104 (2003) 209–216.
[27] M. Sato, T. Kikukawa, T. Araiso, H. Okita, K. Shimono, N. Kamo, M. Demura, K. Nitta, Role of Ser130 and Thr126 in chloride binding and photocycle of *pharaonis* halorhodopsin, Journal of Biochemistry 134 (2003) 151–158.
[28] M. Sato, M. Kubo, T. Aizawa, N. Kamo, T. Kikukawa, K. Nitta, M. Demura, Role of putative anion-binding sites in cytoplasmic and extracellular channels of *Natronomonas pharaonis* halorhodopsin, Biochemistry 44 (2005) 4775–4784.
[29] M. Kubo, T. Kikukawa, S. Miyauchi, A. Seki, M. Kamiya, T. Aizawa, K. Kawano, N. Kamo, M. Demura, Role of Arg123 in light-driven anion pump mechanisms of *pharaonis* halorhodopsin, Photochemistry and Photobiology 85 (2009) 547–555.
[30] M. Iwamoto, C. Hasegawa, Y. Sudo, K. Shimono, T. Araiso, N. Kamo, Proton release and uptake of *pharaonis* phoborhodopsin (sensory rhodopsin II) reconstituted into phospholipids, Biochemistry 43 (2004) 3195–3203.

[31] J. Tamogami, T. Kikukawa, S. Miyauchi, E. Muneyuki, N. Kamo, A tin oxide transparent electrode provides the means for rapid time-resolved pH measurements: application to photoinduced proton transfer of bacteriorhodopsin and proteorhodopsin, Photochemistry and Photobiology 85 (2009) 578–589.
[32] J.K. Lanyi, A. Duschl, G. Váro, L. Zimányi, Anion binding to the chloride pump, halorhodopsin, and its implications for the transport mechanism, FEBS Letters 265 (1990) 1–6.
[33] J. Sasaki, L.S. Brown, Y.S. Chon, H. Kandori, A. Maeda, R. Needleman, J.K. Lanyi, Conversion of bacteriorhodopsin into a chloride ion pump, Science 269 (1995) 73–75.
[34] I.V. Kalaidzidis, A.D. Kaulen, Cl–dependent photovoltage responses of bacteriorhodopsin: comparison of the D85T and D85S mutants and wild-type acid purple form, FEBS Letters 418 (1997) 239–242.
[35] J. Tittor, U. Haupts, C. Haupts, D. Oesterhelt, A. Becker, E. Bamberg, Chloride and proton transport in bacteriorhodopsin mutant D85T: different modes of ion translocation in a retinal protein, Journal of Molecular Biology 271 (1997) 405–416.
[36] S. Rouhani, J.P. Cartailler, M.T. Facciotti, P. Walian, R. Needleman, J.K. Lanyi, R.M. Glaeser, H. Luecke, Crystal structure of the D85S mutant of bacteriorhodopsin: model of an O-like photocycle intermediate, Journal of Molecular Biology 313 (2001) 615–628.
[37] M.T. Facciotti, V.S. Cheung, D. Nguyen, S. Rouhani, R.M. Glaeser, Crystal structure of the bromide-bound D85S mutant of bacteriorhodopsin: principles of ion pumping, Biophysical Journal 85 (2003) 451–458.
[38] M.T. Facciotti, V.S. Cheung, C.S. Lunde, S. Rouhani, N.S. Baliga, R.M. Glaeser, Specificity of anion binding in the substrate pocket of bacteriorhodopsin, Biochemistry 43 (2004) 4934–4943.
[39] M. Rüdiger, D. Oesterhelt, Specific arginine and threonine residues control anion binding and transport in the light-driven chloride pump halorhodopsin, EMBO Journal 16 (1997) 3813–3821.
[40] A. Seki, S. Miyauchi, S. Hayashi, T. Kikukawa, M. Kubo, M. Demura, V. Ganapathy, N. Kamo, Heterologous expression of *pharaonis* halorhodopsin in *Xenopus laevis* oocytes and electrophysiological characterization of its light-driven Cl^- pump activity, Biophysical Journal 92 (2007) 2559–2569.
[41] G. Váró, L.S. Brown, R. Needleman, J.K. Lanyi, Proton transport by halorhodopsin, Biochemistry 35 (1996) 6604–6611.